Scripta Materialia 143 (2018) 63–67

Contents lists available at ScienceDirect

Scripta Materialia

journal homepage: www.elsevier.com/locate/scriptamat

Regular article

Unexpected cyclic stress-strain response of dual-phase high-entropy alloys induced by partial reversibility of deformation

Thomas Niendorf [a,*], Thomas Wegener [a], Zhiming Li [b], Dierk Raabe [b]

[a] Universität Kassel, Institut für Werkstofftechnik (Materials Engineering), 34125 Kassel, Germany
[b] Max-Planck-Institut für Eisenforschung, Max-Planck-Straße 1, 40237 Düsseldorf, Germany

ARTICLE INFO

Article history:
Received 29 July 2017
Received in revised form 7 September 2017
Accepted 8 September 2017
Available online xxxx

Keywords:
High-entropy alloy
Fatigue
Dual phase
Planar slip
Martensite

ABSTRACT

The recently developed dual-phase high-entropy alloys are characterized by pronounced strain hardening and high ductility under monotonic loading owing to the associated transformation induced plasticity effect. Fatigue properties of high-entropy alloys have not been studied in depth so far. The current study focuses on the low-cycle fatigue regime. Cyclic tests were conducted and the microstructure evolution was studied post-mortem. Despite deformation-induced martensitic transformation during cycling at given plastic strain amplitudes, intense strain hardening in the cyclic stress-strain response is not observed. This behavior is attributed to the planar nature of slip and partial reversibility of deformation.

The development of new alloys combining high strength with excellent ductility has stimulated numerous research activities in recent years, mostly focusing on steels. High-Mn steels have led to considerable advances in recent years [1–5]. Through compositional tuning, the stacking fault energy (SFE) can be tailored for two deformation effects, namely, twinning induced plasticity (TWIP) and transformation induced plasticity (TRIP). Depending on the actual value of the SFE, being affected by chemical composition and temperature, either mechanical twinning or martensitic transformation are prevalent besides planar dislocation slip [2,3,5,6–9]. Dislocation-twin and dislocation-phase boundary interactions lead to high strain hardening reserves and delayed necking under monotonic loading [1–5,10–13].

Recently, interest has increased in similar strain hardening effects observed in high-entropy alloys (HEAs). Primarily, these alloys, also referred to as multi-component alloys or compositionally complex alloys, are composed by at least five elements in equiatomic composition [14]. This concept is different from earlier alloying philosophies which typically use only one dominant base element [1–13]. Due to this principal difference in the alloy design approach also non-equiatomic alloys consisting of only four main elements are in the literature often referred to as HEA such as the alloy studied here [15].

Mainly two groups of HEAs have been characterized quite comprehensively, viz. refractory HEAs and HEAs composed by group-IV transition elements [16,17]. Within the latter group the well-known single phase Cantor-alloy, i.e. Fe-Mn-Ni-Co-Cr, has been studied in some detail, particularly focusing on the deformation behavior and fracture toughness at cryogenic temperatures [18–20]. Deformation in the Fe-Mn-Ni-Co-Cr system is characterized by dislocation slip and twinning, the latter becoming more prevalent in the cryogenic regime [18,20]. Thus, some similarities between the behavior of high-Mn TWIP steels and the Fe-Mn-Ni-Co-Cr HEA are obvious [21–23]. The material studied here is a $Fe_{50}Mn_{30}Co_{10}Cr_{10}$ alloy, characterized by a two phase microstructure obtained after thermo-mechanical processing including quenching from final annealing temperature [15]. Upon tensile straining the metastable face-centered cubic (fcc) phase shows a martensitic transformation to the ε-hexagonal closed packed (hcp) martensite phase. Following monotonic deformation to a local engineering strain of about 65%, the fraction of martensite increases to about 85%. Concomitantly, intense strain hardening is observed. Detailed analysis of the microstructure revealed stacking faults, dislocations patterns, mechanical twins and ε-martensite [15].

These results document the rapid progress in alloy development regarding better understanding and tuning of the monotonic deformation behavior of HEAs. However, when in service, engineering alloys are usually not loaded monotonously but in a non-monotonic fashion. Yet, currently no data reporting on the cyclic behavior and concurrent microstructure evolution in HEAs in the low-cycle fatigue (LCF) regime are available. Only three studies reporting on $Al_{0.5}CoCrCuFeNi$, tested under four-point bending fatigue loading [24,25] and $Al_{0.1}CoCrFeNi$, also tested under bending loading [26], provide first insights into this important topic. All these studies focus on the fatigue strength of the alloys and, thus, on the high-cycle fatigue (HCF) regime, as is also emphasized in current reviews reporting on HEAs [17,27,28]. Generally, in LCF

* Corresponding author.
E-mail address: niendorf@uni-kassel.de (T. Niendorf).

http://dx.doi.org/10.1016/j.scriptamat.2017.09.013
1359-6462/

and HCF regimes different loading conditions are considered, i.e. strain and stress controlled testing, respectively, and, thus, microstructure evolution is significantly different.

From high-Mn steels it is known that microstructure evolution under either monotonic or cyclic loading can differ significantly from each other [29–32]. Some of the current authors studied microstructure evolution in various fatigue regimes ranging from LCF to fracture mechanical testing [30,31]. Interestingly, the TWIP steels probed in these studies, i.e. thermo-mechanically processed micro-alloyed Fe-Mn22-C0.6, did not reveal twinning under cyclic loading [31]. Only re-arrangement of dislocation structures was observed under cyclic loading at room temperature (RT) [31]. Thus, counter-intuitively, high accumulated strains led to cyclic softening instead of cyclic hardening as would have been expected from the monotonic deformation behavior. Only monotonic pre-deformation, prior to cyclic loading, was able to stabilize fatigue response due to increase in twin density and, thus, intensified twin-dislocation interactions [31].

The current study aims at providing first insights into the microstructure evolution of dual-phase HEAs under cyclic loading. Testing at RT in the LCF regime is accompanied by microstructure characterization employing X-ray diffraction and electron microscopy. The results reveal an unexpected microstructure upon testing: despite significant evolution of strain induced martensite, hardly any associated strain hardening is observed during cycling up to about 90,000 cycles at low strain amplitude of $\Delta\varepsilon/2 = 0.23\%$ and 10,000 cycles at high strain amplitude of $\Delta\varepsilon/2 = 0.6\%$, i.e. accumulated plastic strains of well above 1000% in all cyclic tests conducted. The ε-martensite fraction of about 95 vol% developing upon fatigue at the within this study studied highest cyclic strain amplitude (0.6%) even exceeds values found upon monotonic testing. The results are discussed based on the underlying deformation characteristics.

The initial ingot was cast in a vacuum induction furnace using pure metals and subsequently thermo-mechanically processed [15]. Two different conditions are probed here. A *fine grained* dual-phase condition has been obtained by annealing at 900 °C followed by water quenching. The second one, referred to as *coarse grained* condition has been subsequently heat treated at 850 °C for 20 min followed by furnace cooling. The coarse grained condition shows hardly any hcp phase in the initial state, i.e. well below 1 vol% according to EBSD and non-detectable in the XRD spectrum (cf. Figs. 1 and 3). Initial martensite fraction for the fine grained condition is about 3 vol% according to EBSD analysis. Samples with gauge section dimensions of 8 mm × 3 mm × 1.5 mm were cut by electro-discharge machining (EDM). In order to remove the affected surface layer all samples were subsequently mechanically ground and polished down to 5 μm grit size. Furthermore, samples were vibration polished using conventional oxide polishing suspension (OPS). Mechanical tests were conducted using a MTS load-rig in fully reversed push-pull loading in strain control. For determination of strains a miniature extensometer featuring a 3 mm gauge length was directly attached to the specimen. Nominal strain rate in all tests was $6 \times 10^{-3}\,s^{-1}$. For phase analysis an X-Ray diffractometer (XRD) equipped with a Cu Kα source operated at 40 kV was used. Microstructure analysis including electron channeling contrast imaging (ECCI) was done using a high-resolution scanning electron microscope (SEM) at acceleration voltage of 30 kV. The SEM employed is equipped with an electron backscatter diffraction (EBSD) unit and a backscattered electron (BSE) detector.

Fig. 1 shows initial microstructures and the cyclic stress responses of the $Fe_{50}Mn_{30}Co_{10}Cr_{10}$ alloy in both conditions in the LCF regime. Most pronounced evolution of microstructure is expected in the LCF regime. Thus, first fatigue tests in the dual-phase TRIP-HEA were conducted under strain controlled conditions at low to relatively high strains. Currently, no results regarding HCF performance of the TRIP-HEA are available, however, will be provided in future studies, amongst others focusing on the role of plastic strain amplitude, strain rate and testing frequency, respectively. Strain amplitudes in current work ranged from $\Delta\varepsilon/2 = 0.23\%$ to $\Delta\varepsilon/2 = 0.6\%$. In order to prevent buckling of the miniature samples the load was increased stepwise during the very first cycles and the final strain amplitude was reached after 50 to 75 cycles depending on the strain amplitude. Thus, the initial cycles are not shown in Fig. 1 for the sake of clarity. The fine grained and the coarse grained TRIP-HEA conditions are characterized by an almost stable stress plateau throughout the tests. Minor strain hardening is only observed for relatively high strain amplitudes. For the strain amplitudes of $\Delta\varepsilon/2 = 0.23\%$ and $\Delta\varepsilon/2 = 0.28\%$ even slight softening is observed in the coarse grained TRIP-HEA (Fig. 1b). As can be seen in Fig. 1a, the fine grained TRIP-HEA is characterized by stable response at the small strain amplitudes (upon initial transient behavior, which cannot be evaluated due to the initial minor loops conducted for avoiding buckling), while for $\Delta\varepsilon/2 = 0.4\%$ and $\Delta\varepsilon/2 = 0.6\%$ slight hardening sets in. Stress amplitudes at a given strain amplitude are higher for the fine grained TRIP-HEA, which is due to the smaller initial grain size. In all cyclic tests for the fine grained and coarse grained conditions the accumulated plastic strain was well above 1000%. The absence of pronounced strain hardening upon cyclic loading as compared to the case of monotonic testing up to local engineering strain of about 65%, where intense strain hardening is observed [15], is striking and will be discussed below. Most importantly, despite the pronounced martensitic transformation found, intense dislocation-phase boundary interactions seem not to be present. From numerous studies focusing on a huge variety

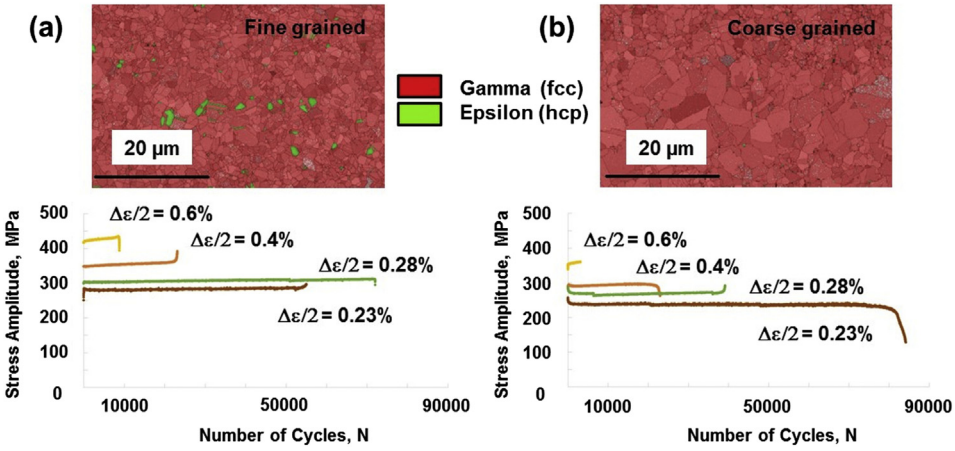

Fig. 1. Cyclic stress response of (a) fine grained (about 5 μm average grain size) and (b) coarse grained (about 10 μm average grain size) TRIP-HEAs tested under various strain amplitudes at room temperature and constant strain rate. The EBSD phase maps highlight differences in the initial microstructural conditions (red: γ-phase, green: ε-phase). (For interpretation of the references to color in this figure legend, the reader is referred to the web version of this article.)

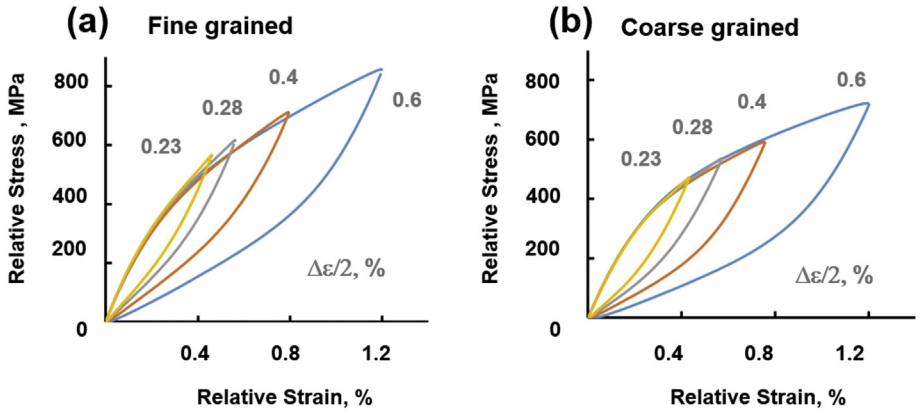

Fig. 2. Hysteresis loops plotted in relative coordinates at half-life for (a) fine grained and (b) coarse grained TRIP-HEA. Similarity of the upper branches of the hysteresis loops for different strain amplitudes reveals perfect Masing behavior for the coarse grained TRIP-HEA (b), the fine grained TRIP-HEA revels slight differences for each amplitude (a).

of metals and alloys it is well known that microstructure evolution and the concomitant course of the stress response in strain controlled fatigue experiments do not produce pronounced scatter. Thus, only one sample per strain amplitude has been tested. Fatigue lives under these loading conditions, however, may be affected by process induced defects. Consequently, differences in fatigue lives are not discussed here as further experiments on a statistical basis are needed at this point and will be subject of future work.

Fig. 2 depicts half-life hysteresis loops plotted in relative coordinates. For all conditions tested the mean stress was below 20 MPa (not shown). For coarse grained (Fig. 2b) TRIP-HEA the upper branches of the hysteresis loops are almost congruent revealing perfect Masing-

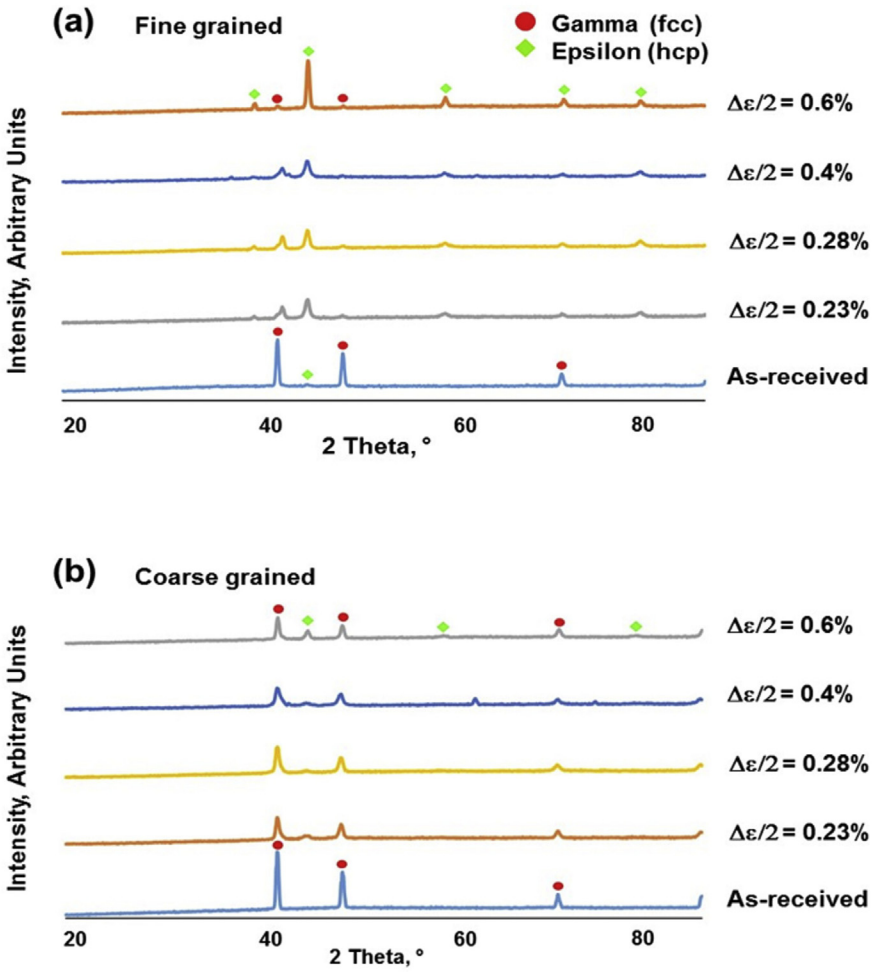

Fig. 3. XRD phase analysis for all conditions tested, in (a) for the fine grained and in (b) for the coarse grained TRIP-HEA. The initial microstructures in (a) and (b) already differ in terms of phase composition. Upon fatigue fraction of the ε-phase (green diamonds) increases while the γ-phase fraction (red circles) decreases. Evolution of phase fraction is most prominent for the fine grained TRIP-HEA at highest strain amplitude. (For interpretation of the references to color in this figure legend, the reader is referred to the web version of this article.)

behavior, i.e. similar microstructure evolution irrespective of the imposed strain amplitude. In contrast, for fine grained (Fig. 2a) TRIP-HEA slight deviations are revealed for the relative hysteresis curves and, thus, non-perfect near-Masing-behavior. Microstructure evolution in this condition is slightly affected by the absolute value of the strain amplitude. However, differences are not pronounced and, thus, can hardly be revealed by microstructure analysis. At first glance the cyclic stress-strain behavior of the TRIP-HEAs seems to be very similar to that of high-Mn TWIP/TRIP steels [31,32]. In these steels, only high-strain monotonic loading leads to the initiation of TRIP and TWIP effects at RT, respectively, and high accumulated cyclic strains alone do not generally lead to twinning and/or martensitic transformation. In consequence, the fatigue response in the LCF regime in these alloys is characterized by the presence of a stable stress plateau [31]. In the present study, planarity of slip seems to be pronounced in the fine grained and the coarse grained TRIP-HEAs. The important role of slip planarity has already been observed in this context in the case of monotonic testing where stacking faults in the fcc phase and twins in the hcp martensitic phase were detected [15]. Alloys featuring planar slip are known to show very similar microstructure evolution irrespective of the strain amplitude applied during cyclic loading. Masing-behavior as observed in Fig. 2 provides clear proof of the planar nature of dislocation motion in the HEA investigated in the current work.

In order to analyze the microstructure evolution, the samples tested have been characterized by XRD and SEM. Results obtained by XRD are shown in Fig. 3, ECCI micrographs and an EBSD phase map are shown in Fig. 4. ECCI and EBSD results are only shown for a single condition TRIP-HEA, tested at $\Delta\varepsilon/2 = 0.6\%$ for the sake of brevity. As for the coarse grained TRIP-HEA depicted, the ECCI and EBSD phase analysis support results provided by XRD phase analysis in all fatigued conditions. The XRD phase analysis shown in Fig. 3 reveals that the initial microstructures of the fine grained and the coarse grained TRIP-HEA samples differ. While the fine grained condition is characterized by a dual-phase microstructure consisting of γ-phase and ε-martensite (in line with [15]), the coarse grained condition only reveals presence of γ-phase. Upon fatigue testing phase fractions change in both conditions, however, more significantly in the fine grained TRIP-HEA (Fig.3a). Decrease of intensity of all γ-peaks (peaks highlighted by red circles) is accompanied by an increase of the intensities of peaks related to the ε-martensite (peaks highlighted by green diamonds). For the fine grained condition tested at $\Delta\varepsilon/2 = 0.6\%$ peaks related to the γ-phase can only hardly be distinguished anymore. Evolution in the coarse grained condition is similar (Fig. 3b), however, a larger fraction of γ-phase seems to prevail. It is important to point out that these XRD data have not been corrected to account for crystallographic texture, thus, a quantitative analysis cannot be provided at this point.

Analysis obtained by ECCI and EBSD further provides clear evidence for martensitic transformation upon cycling (Fig. 4). The overview ECCI micrograph shown in Fig. 4a reveals that the whole sample volume contributes to the overall phase evolution, i.e. traces of martensite appear in all grains depicted. The EBSD phase mapping (Fig. 4b) from the area marked in Fig. 4a reveals that almost the whole volume transformed to ε-martensite. The fraction of martensite deduced from this scan is about 95%. The high-magnification ECCI micrograph (Fig. 4c) taken from a two phase region highlighted in the EBSD map reveals typical features of the ε-martensite at sub-micron scale. These features reveal that the martensite has been formed strain-induced upon mechanical loading, i.e. very similar to corresponding observations on monotonically loaded samples [15].

From the findings presented it can be concluded that the fatigue behavior of the TRIP-HEAs is fundamentally different from that of high-Mn TWIP/TRIP steels, even though the cyclic stress responses in strain controlled tests in the LCF regime look similar at first glance. Microstructure analysis reveals that a very large fraction (up to 95 vol%) of the microstructure transforms to ε-martensite, at least at the highest strain amplitude of 0.6% employed in this study. This transformation, however, does

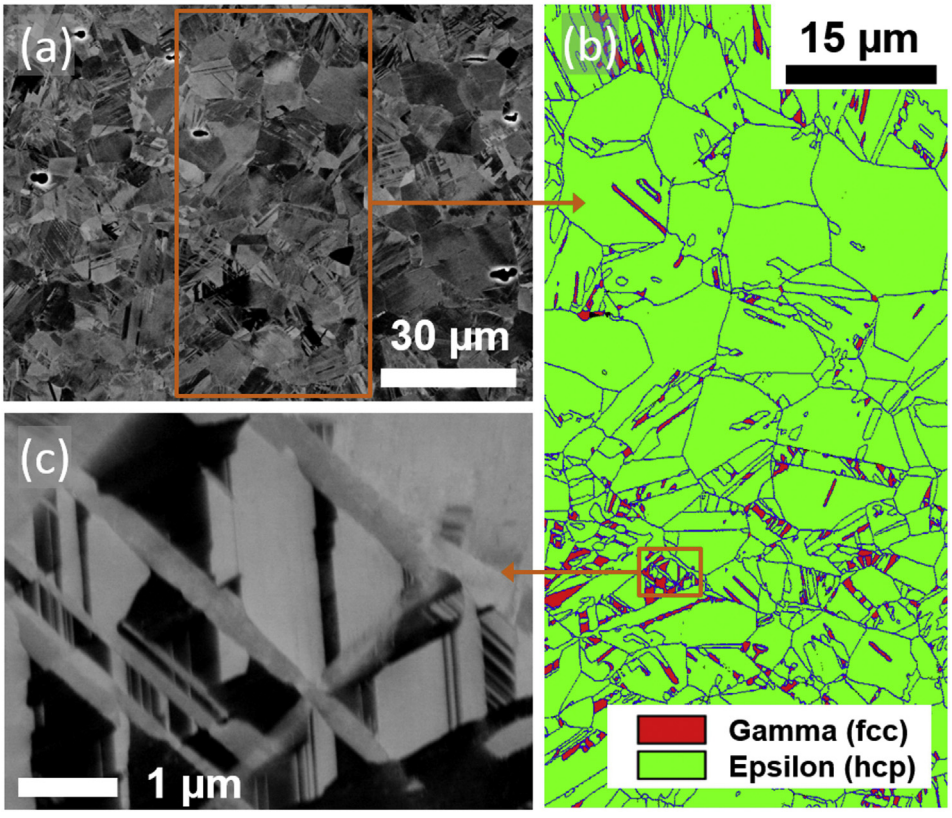

Fig. 4. Microstructure evolution of the coarse grained TRIP-HEA tested at a strain amplitude of $\Delta\varepsilon/2 = 0.6\%$ as characterized by post-mortem (a) and (c) ECCI and (b) EBSD phase analysis. Characterization covers several length scales in order to reveal that microstructure evolution is not a phenomenon induced by local constraints.

interestingly not lead to pronounced cyclic hardening. Planarity of slip as revealed by Masing behavior found for the TRIP-HEA investigated in the current work, is well known from TWIP/TRIP steels. However, this finding is not sufficient for rationalizing the absence of hardening upon cyclic loading. Generally, cyclic plastic deformation, as enforced by fully reversed push-pull LCF loading, is accommodated by several deformation mechanisms being active simultaneously. These mechanisms interact and particularly the martensite is known for its intense interaction with the individual plasticity defects, leading to strain hardening. The current results reveal that hardly any interaction of elementary deformation mechanisms takes place despite significant evolution of ε-martensite in the TRIP-HEA upon cycling. Still, tensile and compressive deformation have to be accommodated. It is concluded, that this deformation can be only accommodated by forward-backward shear, i.e. some degree of reversible deformation. The tests in the LCF regime up to a maximum strain amplitude of 0.6% seem to promote a microplastic stage in the TRIP-HEA that is devoid of too much interaction between ε-martensite, twins and dislocations. Thus, hardening effects seem to be impeded to some extent in the current LCF regime probed, indicating at least partial reversibility of deformation as has been shown e.g. for plasticity in Cu during bending [33]. Simultaneously, ε-martensite formation is promoted by this mechanism in the TRIP-HEA. Even if the aforementioned assumptions are strongly supported by the results presented in the current work, further studies have to be conducted analyzing interaction of elementary deformation mechanisms in depth. These studies will be conducted using samples not only differing in initial grain size, but also in initial martensite volume fraction being induced by monotonic pre-deformation. Studies will include thorough microstructure analysis down to the submicron scale in order to provide evidence for (partial) reversibility of deformation, amongst others using digital image correlation and transmission electron microscopy. These studies will shed light on the role of martensitic transformation and interaction of elementary deformation mechanisms for the specific alloy in focus and HEAs in general.

In summary, cyclic deformation response and corresponding microstructure evolution of $Fe_{50}Mn_{30}Co_{10}Cr_{10}$ TRIP-HEA have been investigated. The effects of initial grain size and phase composition have been evaluated by testing two different conditions. Based on testing in the low-cycle fatigue regime the following conclusions are drawn:

- Deformation mechanisms under monotonic and cyclic loading differ significantly. Under push-pull loading in the LCF regime cyclic hardening is hardly observed at given strain amplitudes. Unexpectedly, pronounced martensitic transformation is found.
- (Near-)Masing-behavior is found for the TRIP-HEA tested. Independent of loading level very similar microstructures form in the two conditions of material probed. Thus, planarity of slip is assumed to strongly affect the material behavior.
- The deformation mechanisms and microstructure evolution of the TRIP-HEA are fundamentally different to that of the otherwise comparable high-Mn TWIP/TRIP steels. Planarity of slip seems to provide for partial reversibility of deformation in the TRIP-HEA.

Experimental support by M. Vollmer and R. Hunke is gratefully acknowledged.

References

[1] O. Grässel, L. Krüger, G. Frommeyer, L.W. Meyer, Int. J. Plast. 16 (2000) 1391.
[2] B.C. De Cooman, Y. Estrin, S.K. Kim, Acta Mater. (2017) (in press).
[3] B.C. De Cooman, in: R. Rana, S.B. Singh (Eds.), Automotive Steels Design, Metallurgy, Processing and Applications, 1st Edition 2017, p. 317.
[4] D.R. Steinmetz, T. Jäpel, B. Wietbrock, P. Eisenlohr, I. Gutierrez-Urrutia, A. Saeed-Akbari, T. Hickel, F. Roters, D. Raabe, Acta Mater. 61 (2013) 494.
[5] O. Bouaziz, S. Allain, C. Scott, P. Cugy, D. Barbier, Curr. Opin. Solid State Mater. Sci. 15 (2011) 141.
[6] S. Allain, J.-P. Chateau, O. Bouaziz, S. Migot, N. Guelton, Mater. Sci. Eng. A 387-389 (2004) 158.
[7] A. Saeed-Akbari, J. Imlau, U. Prahl, W. Bleck, Metall. Mater. Trans. A 40 (2009) 3076.
[8] A. Dumay, J.-P. Chateau, S. Allain, S. Migot, O. Bouaziz, Mater. Sci. Eng. A 483-484 (2008) 184.
[9] E. Welsch, D. Ponge, S.M. Hafez Haghighat, S. Sandlöbes, P. Choi, M. Herbig, S. Zaefferer, D. Raabe, Acta Mater. 116 (2016) 188.
[10] G. Frommeyer, U. Brüx, P. Neumann, ISIJ Int. 43 (2003) 438.
[11] P. Kusakin, A. Belyakov, C. Haase, R. Kaibyshev, D.M. Molodov, Mater. Sci. Eng. A 617 (2014) 52.
[12] I. Gutierrez-Urrutia, D. Raabe, Acta Mater. 59 (2011) 6449.
[13] M. Koyama, T. Sawaguchi, K. Tsuzaki, Mater. Sci. Eng. A 556 (2012) 331.
[14] J.-W. Yeh, S.-K. Chen, S.-J. Lin, J.-Y. Gan, T.-S. Chin, T.-T. Shun, C.-H. Tsau, S.-Y. Chang, Adv. Eng. Mater. 65 (2004) 299.
[15] Z. Li, K.G. Pradeep, Y. Deng, D. Raabe, C.C. Tasan, Nature 534 (2016) 227.
[16] J.-W. Yeh, Ann. Chimie Sci. Materiaux 31 (2006) 633.
[17] D.B. Miracle, O.N. Senkov, Acta Mater. 122 (2017) 448.
[18] F. Otto, A. Dlouhy, C. Somsen, H. Bei, G. Eggler, E.P. George, Acta Mater. 61 (2013) 5743.
[19] N. Stepanov, M. Tikhonovsky, N. Yurchenko, D. Zyabkin, M. Klimova, S. Zherebtsov, A. Efimov, G. Salishchev, Intermetallics 59 (2015) 8.
[20] B. Gludovatz, A. Hohenwarter, D. Catoor, E.H. Chang, E.P. George, R.O. Ritchie, Science 345 (2014) 1153.
[21] D. Raabe, C.C. Tasan, H. Springer, M. Bausch, Steel Research International, 86, 2015 1127.
[22] Y. Deng, C.C. Tasan, K.G. Pradeep, H. Springer, A. Kostka, D. Raabe, Acta Mater. 94 (2015) 124.
[23] K.G. Pradeep, C.C. Tasan, M.J. Yao, Y. Deng, H. Springer, D. Raabe, Mater. Sci. Eng. A 648 (2015) 183.
[24] M.A. Hemphill, T. Yuan, A.M. Wang, J.-W. Yeh, C.-W. Tsai, A. Chuang, P.K. Liaw, Acta Mater. 60 (2012) 5723.
[25] Z. Tang, T. Yuan, C.-W. Tsai, J.-W. Yeh, C.D. Lundin, P.K. Liaw, Acta Mater. 99 (2015) 247.
[26] K. Alagarsamy, A. Fortier, M. Komarasamy, N. Kumar, A. Mohammad, S. Banerjee, H.-C. Han, R.S. Mishra, Cardiovasc. Eng. Technol. 7 (2016) 448.
[27] Y. Zhang, T.T. Zuo, Z. Tang, M.C. Gao, K.A. Dahmen, P.K. Liaw, Z.P. Lu, Prog. Mater. Sci. 61 (2014) 1.
[28] M.-H. Tsai, J.-W. Yeh, Mater. Res. Let. 2 (2014) 107.
[29] A.S. Hamada, L.P. Karjalainen, J. Puustinen, Mater. Sci. Eng. A 517 (2009) 68.
[30] T. Niendorf, F. Rubitschek, H.J. Maier, J. Niendorf, H.A. Richard, A. Frehn, Mater. Sci. Eng. A 527 (2010) 2412.
[31] T. Niendorf, C. Lotze, D. Canadinc, A. Frehn, H.J. Maier, Mater. Sci. Eng. A 499 (2009) 518.
[32] C.W. Shao, P. Zhang, R. Liu, Z.J. Zhang, J.C. Pang, Q.Q. Duan, Z.F. Zhang, Acta Mater. 118 (2016) 196.
[33] E. Demir, D. Raabe, Acta Mater. 58 (2010) 6055.